Electronic Supplementary Material (ESI) for Food & Function.

Supplementary Material

Effect of chitosan second layer on the gelation and controlled digestion of Citrem-chitosan bilayer emulsions

Kunal Kadiya, Manisha Sharma and Supratim Ghosh*

University of Saskatchewan, 51 Campus Drive, Saskatoon, SK S7N 5A8, Canada

*Corresponding author

Email: Supratim.ghosh@usask.ca

Table of Contents

Method S1

Preparation of 50% DDA chitosan by reacetylation

As shown in Equation S1, the original chitosan powder obtained with 93% DDA was chemically transformed into 50% DDA using a reacetylation method described by Vachoud *et al.*[1] and Gatto *et al.*[2]

$$Chitosan\ (DDA\ 93\%) + Acetic\ anhydride \overset{Reacetylation}{\rightarrow} Chitosan\ (DDA\ 50\%) \quad \text{(S1)}$$

First, an aqueous solution of 3 wt% Chitosan DDA 93 was prepared by adding the 3 g chitosan powder (containing [-NH_2] groups) in 97 g of 2wt% aqueous acetic acid [AcA] by considering the stoichiometric proportions of ([AcA] = [-NH_2]) and was stirred overnight. Subsequently, the methanolic solution of chitosan DDA 93 was prepared by mixing an equal amount of chitosan solution and methanol. At first, 90 mL of methanol was added to 100 mL chitosan solution (corresponding to 90% v/v of the chitosan solution) and stirred for 2 h. The other 10 mL methanol (corresponding to 10% v/v of the chitosan solution) was used to prepare the acetic anhydride (AAn) solution for the reacetylation of chitosan DDA 93. The AAn amount (m_{AAn}, g) required to prepare the chitosan with DDA 50 was determined using Equation S2.

$$m_{AAn} = \frac{m_c(DDA_1 - DDA_2)(1 - w_{H_2O})M_{AAn}}{Mw_c} \quad \text{(S2)}$$

Where m_c is the amount of chitosan DDA 93 (g), DDA_1 (0.93) and DDA_2 (0.50) are initial and desired DDAs, respectively, w_{H2O} is moisture content (8 wt%) in the DDA 93 chitosan powder, M_{AAn} is the molecular weight of AAn (102.1 g/mol), and Mw_C is an average molecular weight, calculated using Equation S3, (164.14 g/mol) of the repetitive units of chitosan DDA 93[3]:

$$Mw_c = (0.93 \times M_w\ of\ GlcN) + (0.07 \times M_w\ of\ GlcNAc) \quad \text{(S3)}$$

where, M_w of GlcN and M_w of GlcnAc are the molecular weight of glucosamine and glucosamine acetyl units of chitosan, respectively.

A methanolic solution of AAn was prepared by mixing the calculated amount of AAn, from Equation S2, in 10 mL methanol (corresponding to 10% v/v of the chitosan solution) and was mixed at 400 rpm for 45 minutes. The reacetylation was performed by adding methanolic AAn dropwise to the Chitosan DDA 93 solution and then stirring overnight. The next day, the re-acetylated chitosan with DDA 50 was precipitated using concentrated NH_4OH and filtered out using Whatman filter paper #1 inserted in the 400 mL Buchner funnel. The resultant wet mass was repeatedly washed with distilled water until the water pH reached around 7. After washing, the wet mass was spread onto an aluminium pan and vacuum dried at 50°C till final moisture content reached 6 - 8 wt% in dried chunks. A fine powder was prepared from dried chunks by grinding using mortar and pestle and stored in a desiccator for further DDA analysis.

Method S2

Analysis of Degree of Deacetylation of Chitosan

The degree of deacetylation (DDA) of chitosan DDA 50 and DDA 93 was determined by the pH-conductometric titration method adopted from Crofton *et al.*[4] The pH-conductometric titration was performed by dissolving 100 mg of chitosan powder in the mixture of 90 mL deionized water and 10 mL of 0.1 N HCl. The chitosan solution in 0.1 N HCl was stirred overnight, and the next day it was titrated with 0.1 N NaOH. During the titration, a fixed amount (200 µL) of 0.1 N NaOH was added at a constant rate, and a simultaneous change in the pH and conductivity of solution was recorded with an Orion star A215 pH-Conductivity meter equipped with an Orion conductivity cell and pH electrode. A typical pH-Conductometric titration curve, shown in Fig. S2, was obtained by plotting NaOH volume versus conductivity and pH. The first deflection point appeared in the curve due to an increase in conductivity, indicates the neutralization of excess H^+ ions available in chitosan solution from excess 0.1 N HCl, which is followed by the neutralization of the weak acid, i.e., the ammonium salt in chitosan. The second deflection point indicates the complete neutralization of ammonium, and any further addition of OH^- leads to an increase in conductivity. Hence, the volume of 0.1 N NaOH used between the first and second deflection points correspond to the neutralization of the protonated amino groups of chitosan, which was used to calculate the %DDA of chitosan by following Equation from Crofton *et al.*[4]:

$$\%DDA = \frac{M_{NaOH} \times (v_{2\ -}\ v_1) \times 161.16}{W_{ch}(g)} \quad \text{(S4)}$$

Where W_{ch} is the weight of chitosan powder (g), M_{NaOH} is the molarity (mol/L) of standard NaOH solution, v_2 and v_1 are volumes of NaOH (Litre) used till the second and first deflection point, respectively, and 161.16 g/mol is the molar mass of chitosan.[3]

For the confirmation of DDA in DDA 50 and DDA 93 chitosan samples, the Raman spectra of their functional groups were also collected at room temperature using a Renishaw InVia Reflex Raman microscope in the 500 cm^{-1} to 4000 cm^{-1} spectral range (785 nm solid-state diode laser with a 1200 lines/mm grating system). The instrument wavelength was calibrated at 520 cm^{-1} using an internal Si (110) sample. All the collected spectra were analysed using WiRE 5.3 software (Fig. S3).

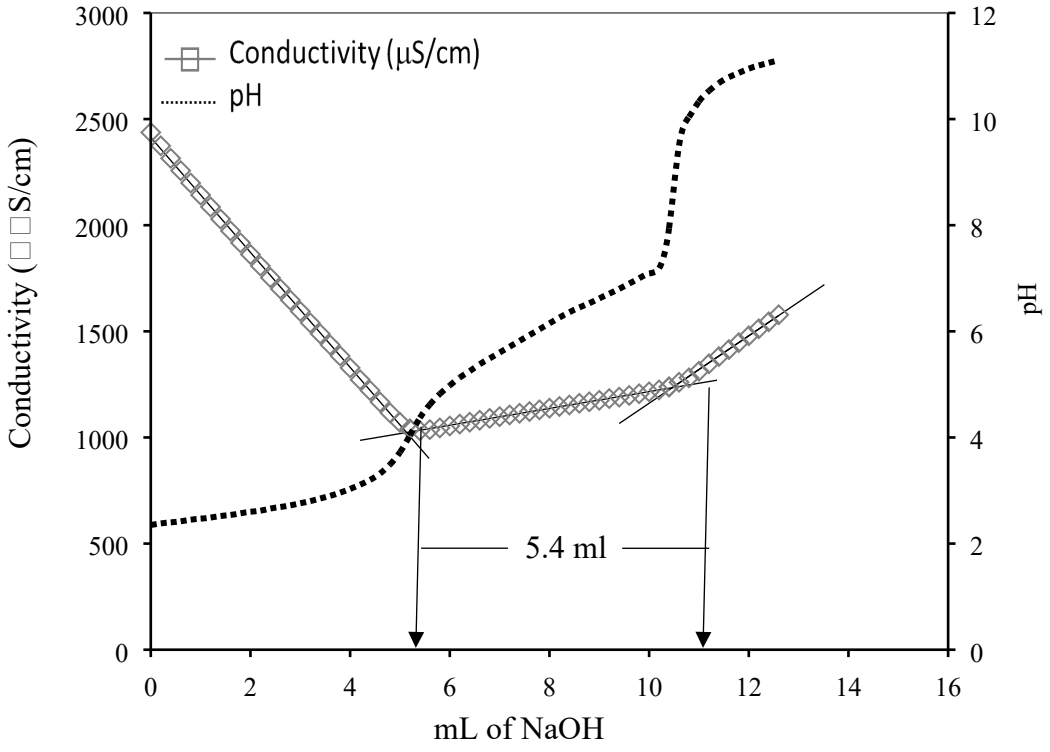

Fig. S1 Analysis of the degree of deacetylation (DDA) of chitosan using the pH-conductometric titration as a function of addition of sodium hydroxide (NaOH).

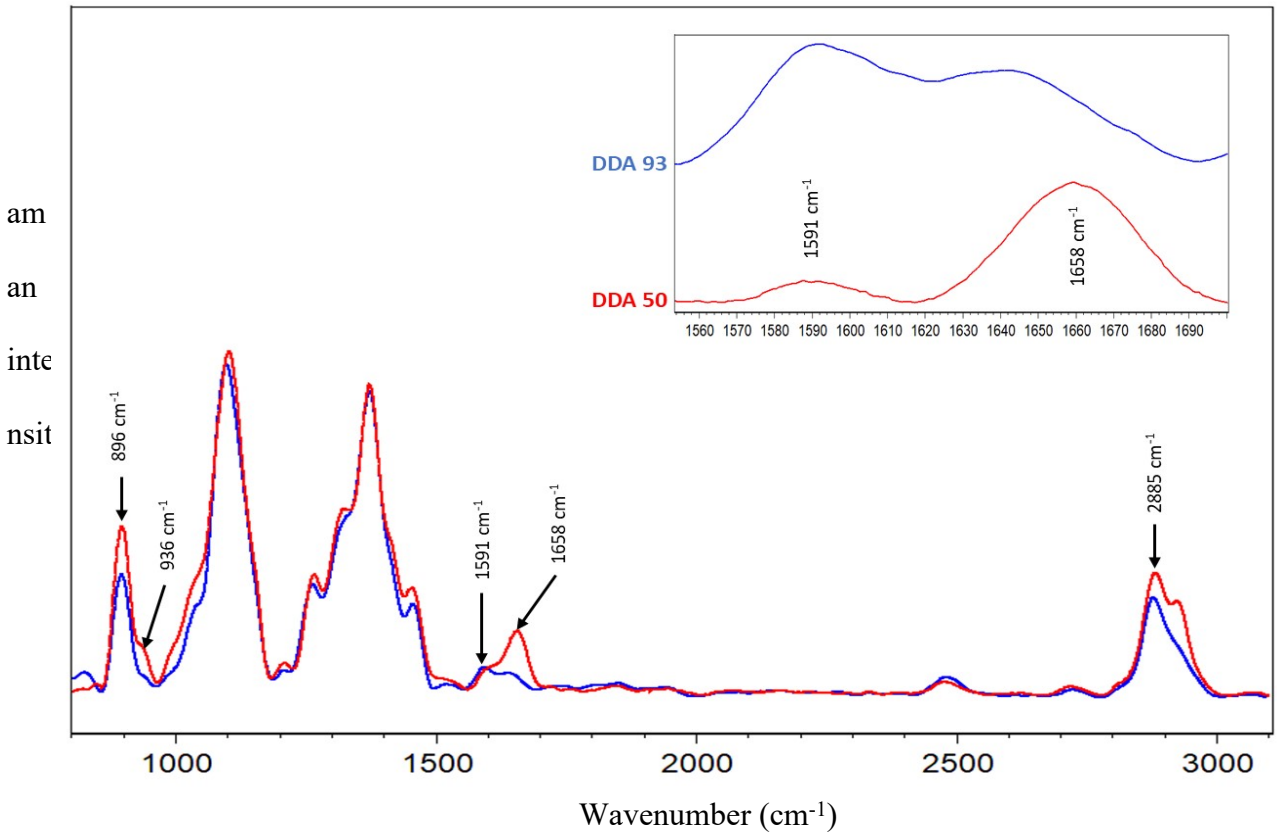

Fig. S2 Raman spectra of chitosan DDA 50 (red) and DDA 93 (blue). The inset shows two peaks at 1591 cm^{-1} and 1658 cm^{-1} for functional groups amide II (NH) and carbonyl (CO).

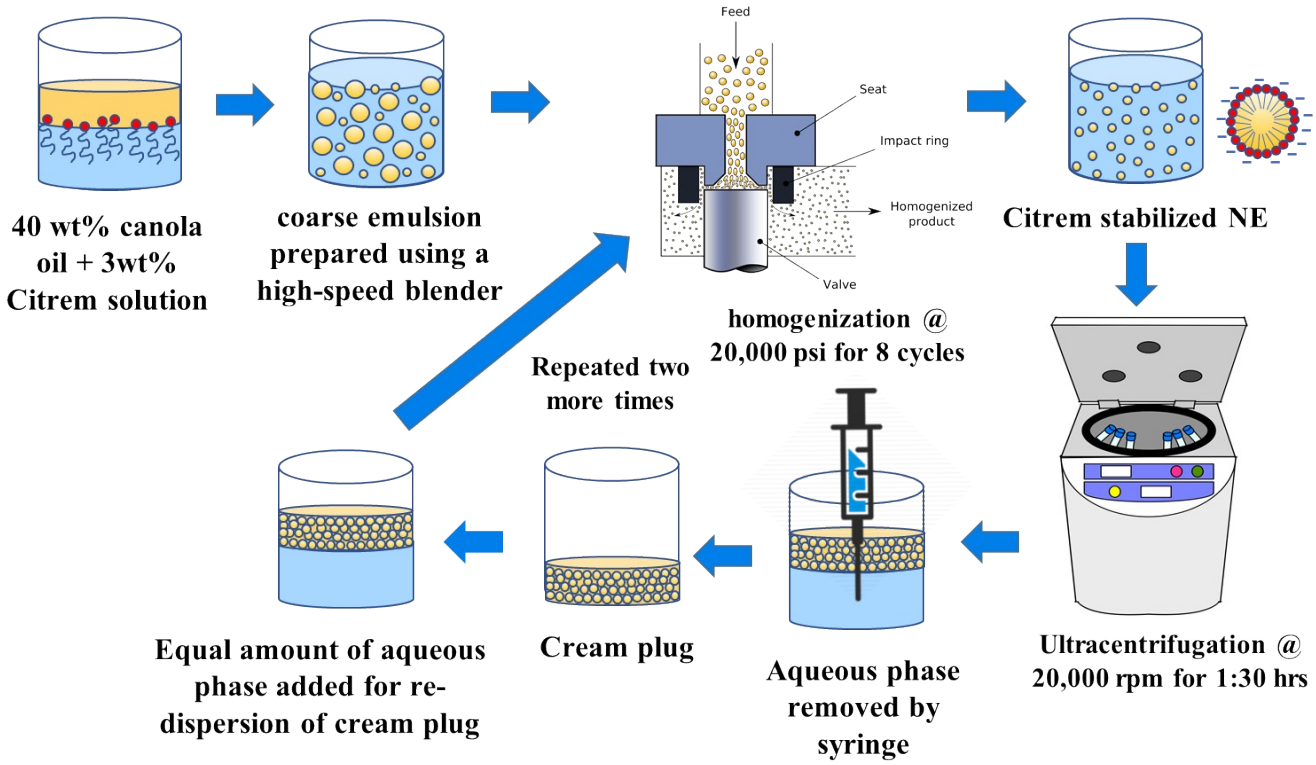

Fig. S3. Preparation of Citrem-stabilized primary emulsion followed by the removal excess emulsifier from the continuous phase of the emulsion by multiple cycles of ultracentrifugation.

Table S1 Formulation for the preparing the Citrem-chitosan bilayer emulsions with different concentration of chitosan DDA 50 and DDA 93.

Concentration of Chitosan (%wt)	**0**	**0.05**	**0.065**	**0.075**	**0.0825**	**0.1**	**0.15**	**0.2**	**0.25**
Quantity of Citrem emulsion (40% oil) at pH 4 (g)	18	18	18	18	18	18	18	18	18
Quantity of 2.5 wt% Chitosan (g)	0	0.4	0.52	0.6	0.66	0.8	1.2	1.6	2
Quantity of acetate buffer pH 4 (g)*	2	1.6	1.48	1.4	1.34	1.2	0.8	0.4	0
Total quantity (g)	20	20	20	20	20	20	20	20	20
wt% Canola oil in final emulsion	36	36	36	36	36	36	36	36	36

**Different amount of acetate buffer was added to keep the final pH and oil concentration of all the bilayer emulsion constant.*

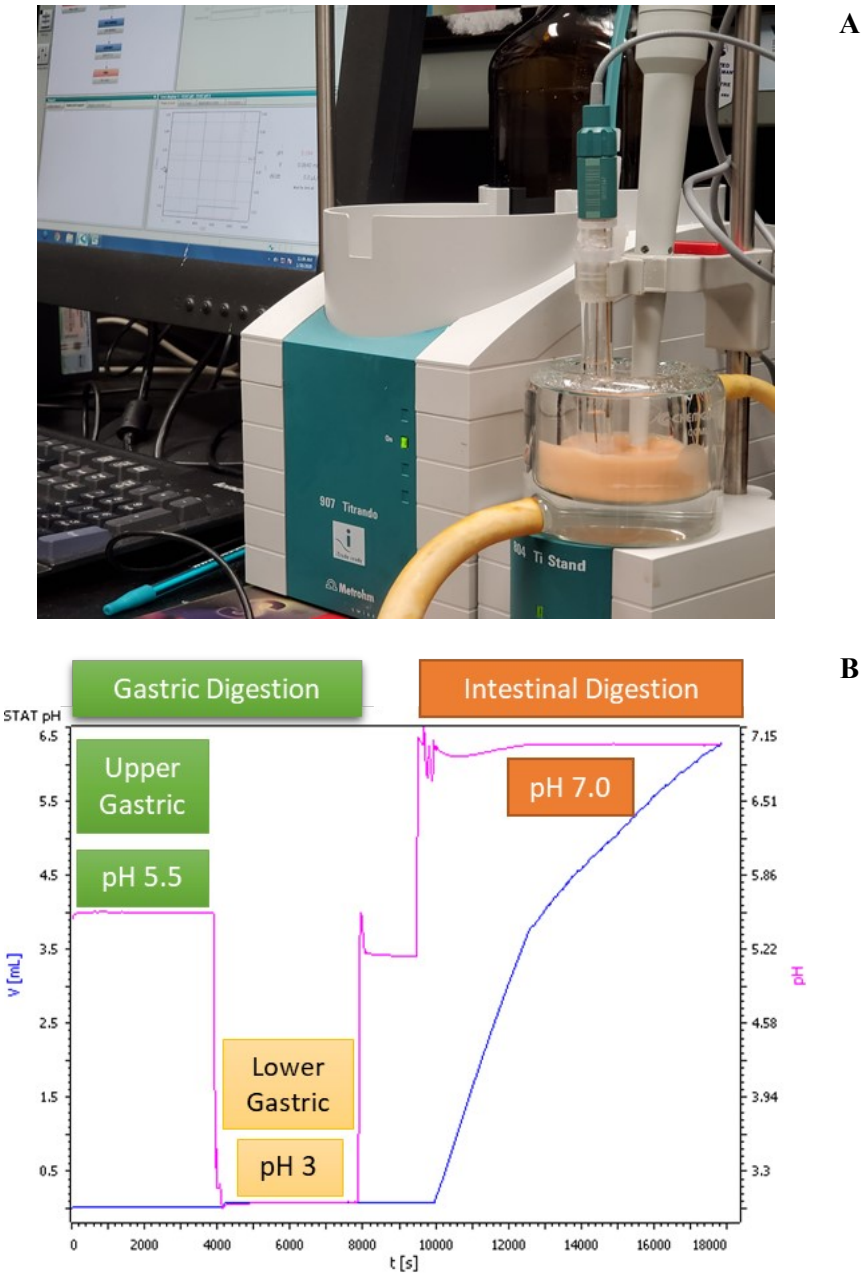

Fig. S4 (A) Static *in vitro* digestion assembly attached to a pH-STAT auto-titrator (B) Output of the pH-STAT digestion kinetics (volume of NaOH added as a function time, blue line) mentioned with the three phases of digestion monitored at different pH values (pink line).

Method S3

Estimation of chitosan layer thickness using dynamic light scattering (DLS)

Dynamic light scattering: The core-shell structure phenomenon and the dynamic light scattering (DLS) technique was used in characterizing the shell-layer thickness of sterically stabilized particles.[5] In the present study, to measure the thickness of the chitosan (DDA 50 and DDA 93) layer, the core-shell structure was created at pH 4 (as shown in Fig. S5). The hydrodynamic diameter of the core Citrem-stabilized emulsion droplets (yellow, Fig. S5) was determined using a DLS instrument (Litesizer™ 500, Anton Paar, Montreal, QC, Canada). The shell layer (green, Fig. S5) was then created by adding chitosan solution at pH 4 to promote electrostatic complexation at the interface between negatively charged Citrem and positively charged chitosan and the hydrodynamic diameter of the bilayer (Citrem + chitosan) droplets was determined. The chitosan shell layer thickness (Δ) was obtained by deducting the Citrem-stabilized droplet (core) size (D_1) from the size of Citrem plus chitosan-stabilized droplets (D_2) (Fig. S5). The chitosan shell layer thickness (Δ) was calculated using Equation S5.

$$\Delta = \frac{D_2 - D_1}{2} \quad \text{(S5)}$$

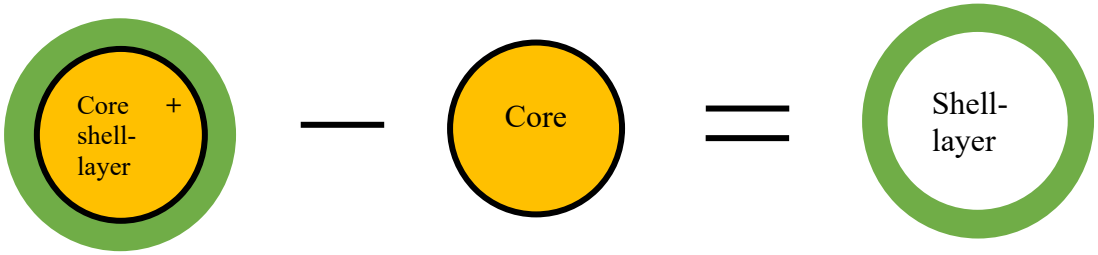

Droplet size (***D₂***) = Citrem-stabilized droplet core + chitosan shell layer

Droplet size (***D₁***) = Citrem-stabilized droplet core

Chitosan shell layer (**2Δ**)

Fig. S5 Schematics of chitosan shell layer thickness measurement from the hydrodynamic diameter of Citrem plus chitosan-stabilized droplets minus the Citrem-stabilized droplets.

Table S2 Estimation of chitosan shell layer thickness using the dynamic light scattering measurements considering the core-shell structure of the bilayer droplets using Equation S5

Chitosan sample	Core + shell, D_2 (nm)	Core, D_1 (nm)	Chitosan shell-layer thickness (Δ) (nm)
DDA 50%	388.9 ± 6.9	216.2 ± 3.8	86.35 ± 3.96
DDA 93%	366.5 ± 2.8	216.2 ± 3.8	75.16 ± 0.62

Method S4

Determination of effective oil volume fraction for mono- and bilayer emulsions

The volume fraction of the shell layer (ϕ_s) as a function of droplet size (r) and shell layer thickness (δ) can be calculated using Equation S6.

$$\phi_s = 1 - \frac{r^3}{(r+\delta)^3} \quad \text{(S6)}$$

Here, δ is the interfacial repulsive shell layer thickness contributed by the charge cloud alone in case of ionic emulsifier (Cirem-stabilized monolayer emulsions) or the charge cloud plus the steric barrier (Cirem-chitosan-stabilized bilayer emulsions) around the droplet in case of the multilayer emulsions. Based on our previous work, the shell layer thickness of Cirem-stabilized monolayer emulsion was calculated using Equations S7 and S8.[6]

$$\delta = 2.9\ \kappa^{-1} \quad \text{(S7)}$$

Debye length, $\kappa^{-1} = 0.304/\sqrt{C}$; C is the molar ionic concentration (S8)

Here, the factor 2.9 was obtained from our previously published data on DLVO calculation for 3 wt% Citrem-stabilized emulsions.[6] To calculate the Debye length, the molar ionic concentration of free sodium and chloride ions present in the emulsion continuous phase was determined by using a NaCl conductivity calibration curve following the methodology by Kadiya and Ghosh (2019). Finally, the overall repulsive barrier (δ) around a bilayer droplet was calculated from the combined effect of charge cloud (x) plus the steric barrier (Δ) according to Patel e*t al.*[7] The calculated and experimentally

determined values of shell layer thickness for both mono- and multi-layer emulsions and the predicted ϕ_s and ϕ_{eff} are reported in Table S3.

Table S3 Predicted values of volume fraction of the shell layer (ϕ_S) and effective oil volume fraction (ϕ_{eff}) for Citrem-stabilized monolayer and Citrem-chitosan-stabilized bilayer droplets calculated from the average droplet size and the values of repulsive charge cloud and steric layer thickness.

Emulsion and chitosan type	Droplet radius, r (nm)	Counterion conc. (mol m^{-3})[§]	Debye length, κ^{-1} (nm)	Repulsive charge cloud thickness $2.9\kappa^{-1}$ (x nm)	Steric layer thickness (Δ nm)	Shell layer thickness, $\delta = x + \Delta$ (nm)	volume fraction of shell layer (ϕ_S)	Effective oil volume fraction[♣] $\phi_{eff} = \phi_{oil} + \phi_s$
Monolayer emulsion	242.0	14.08	2.56	7.43	-	7.43[#]	0.09	0.47
Bilayer emulsion (DDA 50)	1714.9[⌘]	17.24	2.32	6.71	86.35[**]	93.06[*]	0.15	0.53
Bilayer emulsion (DDA 93)	695.7[⌘]	18.33	2.25	6.52	75.16[**]	81.68[*]	0.28	0.66

[⌘]Droplet/ aggregate radius (r) of bilayer emulsions considered without steric barrier (Δ), $r = (d_{32}/2) - \Delta$.

[§]Counter ion concentration was calculated from the molar ionic concentration in the emulsion continuous phase

[#]δ for monolayer emulsion was determined from the repulsive charge cloud using Equation S7.

[*]δ for bilayer emulsion is the sum of electrostatic (x) and steric (Δ) repulsion between the droplets.

[**]The steric layer thickness (Δ) is obtained from Table S2 using Method S3.

[♣]36 wt% oil used in emulsion preparation is equivalent to 0.38 oil volume fraction ($\phi_{oil} = 0.38$).

Method S5

Cryo-scanning electron microscopy

Freeze-fracture Cryo-SEM was also used to investigate the microstructure of polymer encapsulated droplets, and to get an estimation of the thickness of shell wall.[8, 9] In this study, the microstructure of the emulsion droplets with chitosan shell layer was observed by freeze fracturing a small amount of emulsion sample in the cryo-preparation chamber (PP3010T Cryo-SEM preparation system, Quorum Technologies, UK) using liquid nitrogen at -70°C. Then, the freeze fractured sample was sputter-coated with platinum and imaged using JEOL JSM 7100F SEM (JEOL Ltd., Tokyo, Japan) under high vacuum and at an accelerated voltage of 3 keV. The SEM experiment was performed at the Ghent University, Belgium. From the cryo-SEM image, an approximate thickness of chitosan DDA 93 can be sees as 75 nm, which matched quite well with shell-layer thickness from the DLS experiment.

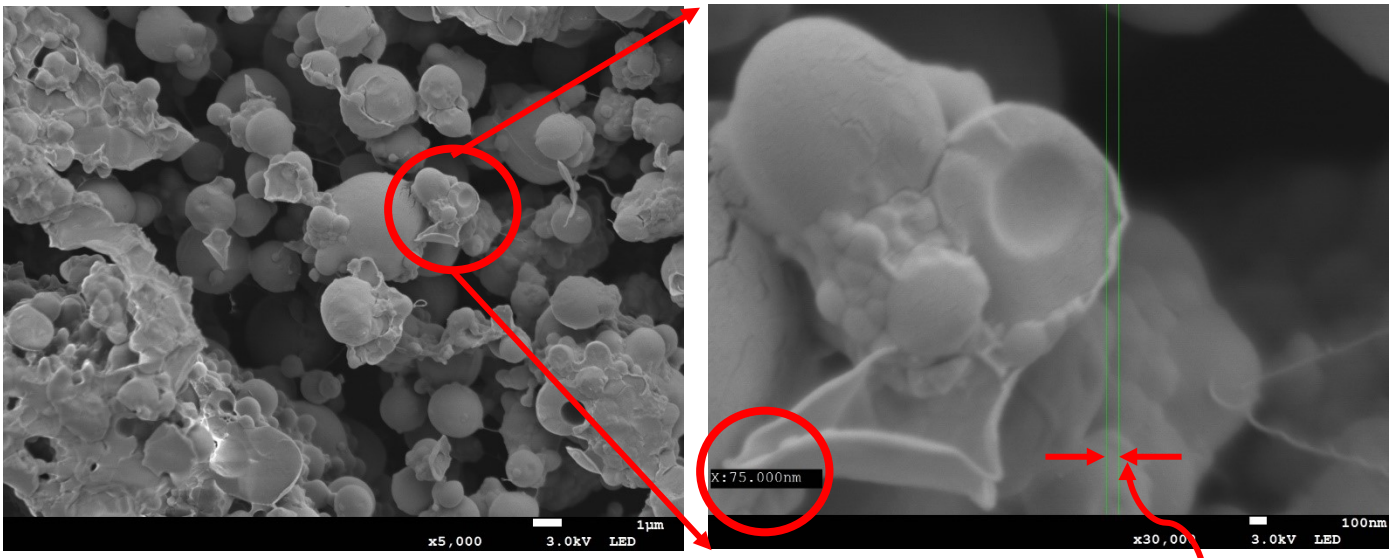

Fig. S6 Cryo-SEM microstructure of Citrem plus chitosan-stabilized bilayer emulsions for the demonstration of chitosan shell-layer thickness

References

1. L. Vachoud, N. Zydowicz and A. Domard, Formation and characterisation of a physical chitin gel, *Carbohydrate research*, 1997, **302**, 169-177.
2. M. Gatto, D. Ochi, C. M. P. Yoshida and C. F. da Silva, Study of chitosan with different degrees of acetylation as cardboard paper coating, *Carbohydrate polymers*, 2019, **210**, 56-63.
3. P. L. Ma, M. Lavertu, F. M. Winnik and M. D. Buschmann, New Insights into chitosan− DNA interactions using isothermal titration microcalorimetry, *Biomacromolecules*, 2009, **10**, 1490-1499.
4. A. R. Crofton, S. M. Hudson, K. Howard, T. Pender, A. Abdelgawad, D. Wolski and W. M. Kirsch, Formulation and characterization of a plasma sterilized, pharmaceutical grade chitosan powder, *Carbohydrate polymers*, 2016, **146**, 420-426.
5. B. Akpinar, L. A. Fielding, V. J. Cunningham, Y. Ning, O. O. Mykhaylyk, P. W. Fowler and S. P. Armes, Determining the effective density and stabilizer layer thickness of sterically stabilized nanoparticles, *Macromolecules*, 2016, **49**, 5160-5171.
6. K. Kadiya and S. Ghosh, Conversion of Viscous Oil-in-Water Nanoemulsions to Viscoelastic Gels upon Removal of Excess Ionic Emulsifier, *Langmuir*, 2019, **35**, 17061-17074.
7. A. Patel, A. Mohanan and S. Ghosh, Effect of protein type, concentration and oil droplet size on the formation of repulsively jammed elastic nanoemulsion gels, *Soft matter*, 2019, **15**, 9762-9775.
8. N.-P. K. Humblet-Hua, E. van der Linden and L. M. Sagis, Microcapsules with protein fibril reinforced shells: effect of fibril properties on mechanical strength of the shell, *Journal of agricultural and food chemistry*, 2012, **60**, 9502-9511.
9. N. Xiang, Y. Lyu and G. Narsimhan, Characterization of fish oil in water emulsion produced by layer by layer deposition of soy β-conglycinin and high methoxyl pectin, *Food Hydrocolloids*, 2016, **52**, 678-689.